

Observation of $\Xi(1620)^0$ and Evidence for $\Xi(1690)^0$ in $\Xi_c^+ \rightarrow \Xi^- \pi^+ \pi^+$ Decays

M. Sumihama,^{13,72} I. Adachi,^{19,15} J. K. Ahn,³⁹ H. Aihara,⁸⁷ S. Al Said,^{81,37} D. M. Asner,³ H. Atmacan,⁷⁷ T. Aushev,⁵⁴ R. Ayad,⁸¹ V. Babu,⁸² I. Badhrees,^{81,36} S. Bahinipati,²³ A. M. Bakich,⁸⁰ V. Bansal,⁶⁷ C. Beleño,¹⁴ M. Berger,⁷⁸ V. Bhardwaj,²² B. Bhuyan,²⁴ T. Bilka,⁵ J. Biswal,³⁴ G. Bonvicini,⁹¹ A. Bozek,⁶² M. Bračko,^{48,34} T. E. Browder,¹⁸ D. Červenkov,⁵ V. Chekelian,⁴⁹ A. Chen,⁵⁹ B. G. Cheon,¹⁷ K. Chilikin,⁴⁴ K. Cho,³⁸ S.-K. Choi,¹⁶ Y. Choi,⁷⁹ S. Choudhury,²⁵ D. Cinabro,⁹¹ S. Cunliffe,⁸ T. Czank,⁸⁵ N. Dash,²³ S. Di Carlo,⁴² Z. Doležal,⁵ T. V. Dong,^{19,15} Z. Drásal,⁵ S. Eidelman,^{4,65,44} D. Epifanov,^{4,65} J. E. Fast,⁶⁷ B. G. Fulsom,⁶⁷ R. Garg,⁶⁸ V. Gaur,⁹⁰ N. Gabyshev,^{4,65} A. Garmash,^{4,65} M. Gelb,³⁵ A. Giri,²⁵ P. Goldenzweig,³⁵ E. Guido,³² J. Haba,^{19,15} K. Hayasaka,⁶⁴ H. Hayashii,⁵⁸ S. Hirose,⁵⁵ W.-S. Hou,⁶¹ K. Inami,⁵⁵ G. Inguglia,⁸ A. Ishikawa,⁸⁵ R. Itoh,^{19,15} M. Iwasaki,⁶⁶ Y. Iwasaki,¹⁹ W. W. Jacobs,²⁷ H. B. Jeon,⁴¹ S. Jia,² Y. Jin,⁸⁷ K. K. Joo,⁶ T. Julius,⁵⁰ A. B. Kaliyar,²⁶ K. H. Kang,⁴¹ G. Karyan,⁸ Y. Kato,⁵⁶ C. Kiesling,⁴⁹ D. Y. Kim,⁷⁶ J. B. Kim,³⁹ K. T. Kim,³⁹ S. H. Kim,¹⁷ K. Kinoshita,⁷ P. Kodyš,⁵ S. Korpar,^{48,34} D. Kotchetkov,¹⁸ P. Križan,^{45,34} R. Kroeger,⁵¹ P. Krokovny,^{4,65} R. Kumar,⁷¹ A. Kuzmin,^{4,65} Y.-J. Kwon,⁹³ J. S. Lange,¹² I. S. Lee,¹⁷ S. C. Lee,⁴¹ L. K. Li,²⁸ Y. B. Li,⁶⁹ L. Li Gioi,⁴⁹ J. Libby,²⁶ D. Liventsev,^{90,19} M. Lubej,³⁴ T. Luo,¹¹ M. Masuda,⁸⁶ T. Matsuda,⁵² D. Matvienko,^{4,65,44} M. Merola,^{31,57} K. Miyabayashi,⁵⁸ H. Miyata,⁶⁴ R. Mizuk,^{44,53,54} G. B. Mohanty,⁸² H. K. Moon,³⁹ T. Mori,⁵⁵ R. Mussa,³² E. Nakano,⁶⁶ T. Nakano,⁷² M. Nakao,^{19,15} T. Nanut,³⁴ K. J. Nath,²⁴ Z. Natkaniec,⁶² M. Niiyama,⁴⁰ N. K. Nisar,⁷⁰ S. Nishida,^{19,15} H. Ono,^{63,64} P. Pakhlov,^{44,53} G. Pakhlova,^{44,54} B. Pal,³ S. Pardi,³¹ H. Park,⁴¹ S. Paul,⁸⁴ T. K. Pedlar,⁴⁷ R. Pestotnik,³⁴ L. E. Piilonen,⁹⁰ V. Popov,^{44,54} M. Ritter,⁴⁶ G. Russo,³¹ D. Sahoo,⁸² S. Sandilya,⁷ L. Santelj,¹⁹ T. Sanuki,⁸⁵ V. Savinov,⁷⁰ O. Schneider,⁴³ G. Schnell,^{1,21} C. Schwanda,²⁹ Y. Seino,⁶⁴ K. Senyo,⁹² M. E. Sevier,⁵⁰ V. Shebalin,^{4,65} C. P. Shen,² T.-A. Shibata,⁸⁸ J.-G. Shiu,⁶¹ B. Shwartz,^{4,65} F. Simon,^{49,83} A. Sokolov,³⁰ E. Solovieva,^{44,54} M. Starič,³⁴ J. F. Strube,⁶⁷ T. Sumiyoshi,⁸⁹ M. Takizawa,^{75,20,73} U. Tamponi,³² K. Tanida,³³ N. Taniguchi,¹⁹ F. Tenchini,⁵⁰ M. Uchida,⁸⁸ T. Uglov,^{44,54} S. Uno,^{19,15} P. Urquijo,⁵⁰ S. E. Vahsen,¹⁸ C. Van Hulse,¹ G. Varner,¹⁸ V. Vorobyev,^{4,65,44} A. Vossen,⁷⁸ B. Wang,⁷ C. H. Wang,⁶⁰ M.-Z. Wang,⁶¹ P. Wang,²⁸ X. L. Wang,¹¹ M. Watanabe,⁶⁴ S. Watanuki,⁸⁵ E. Widmann,⁷⁸ E. Won,³⁹ H. Ye,⁸ J. Yelton,¹⁰ C. Z. Yuan,²⁸ Y. Yusa,⁶⁴ S. Zakharov,^{44,54} Z. P. Zhang,⁷⁴ V. Zhilich,^{4,65} V. Zhukova,^{44,53} and V. Zhulanov^{4,65}

(Belle Collaboration)

¹University of the Basque Country UPV/EHU, 48080 Bilbao²Beihang University, Beijing 100191³Brookhaven National Laboratory, Upton, New York 11973⁴Budker Institute of Nuclear Physics SB RAS, Novosibirsk 630090⁵Faculty of Mathematics and Physics, Charles University, 121 16 Prague⁶Chonnam National University, Kwangju 660-701⁷University of Cincinnati, Cincinnati, Ohio 45221⁸Deutsches Elektronen-Synchrotron, 22607 Hamburg⁹Duke University, Durham, North Carolina 27708¹⁰University of Florida, Gainesville, Florida 32611¹¹Key Laboratory of Nuclear Physics and Ion-beam Application (MOE) and Institute of Modern Physics, Fudan University, Shanghai 200443¹²Justus-Liebig-Universität Gießen, 35392 Gießen¹³Gifu University, Gifu 501-1193¹⁴II. Physikalisches Institut, Georg-August-Universität Göttingen, 37073 Göttingen¹⁵SOKENDAI (The Graduate University for Advanced Studies), Hayama 240-0193¹⁶Gyeongsang National University, Chinju 660-701¹⁷Hanyang University, Seoul 133-791¹⁸University of Hawaii, Honolulu, Hawaii 96822¹⁹High Energy Accelerator Research Organization (KEK), Tsukuba 305-0801²⁰J-PARC Branch, KEK Theory Center, High Energy Accelerator Research Organization (KEK), Tsukuba 305-0801²¹IKERBASQUE, Basque Foundation for Science, 48013 Bilbao²²Indian Institute of Science Education and Research Mohali, SAS Nagar, Mohali 140306²³Indian Institute of Technology Bhubaneswar, Satya Nagar 751007²⁴Indian Institute of Technology Guwahati, Assam 781039²⁵Indian Institute of Technology Hyderabad, Telangana 502285²⁶Indian Institute of Technology Madras, Chennai 600036

- ²⁷*Indiana University, Bloomington, Indiana 47408*
- ²⁸*Institute of High Energy Physics, Chinese Academy of Sciences, Beijing 100049*
- ²⁹*Institute of High Energy Physics, Vienna 1050*
- ³⁰*Institute for High Energy Physics, Protvino 142281*
- ³¹*INFN—Sezione di Napoli, 80126 Napoli*
- ³²*INFN—Sezione di Torino, 10125 Torino*
- ³³*Advanced Science Research Center, Japan Atomic Energy Agency, Naka 319-1195*
- ³⁴*J. Stefan Institute, 1000 Ljubljana*
- ³⁵*Institut für Experimentelle Teilchenphysik, Karlsruher Institut für Technologie, 76131 Karlsruhe*
- ³⁶*King Abdulaziz City for Science and Technology, Riyadh 11442*
- ³⁷*Department of Physics, Faculty of Science, King Abdulaziz University, Jeddah 21589*
- ³⁸*Korea Institute of Science and Technology Information, Daejeon 305-806*
- ³⁹*Korea University, Seoul 136-713*
- ⁴⁰*Kyoto University, Kyoto 606-8502*
- ⁴¹*Kyungpook National University, Daegu 702-701*
- ⁴²*LAL, Univ. Paris-Sud, CNRS/IN2P3, Université Paris-Saclay, Orsay*
- ⁴³*École Polytechnique Fédérale de Lausanne (EPFL), Lausanne 1015*
- ⁴⁴*P.N. Lebedev Physical Institute of the Russian Academy of Sciences, Moscow 119991*
- ⁴⁵*Faculty of Mathematics and Physics, University of Ljubljana, 1000 Ljubljana*
- ⁴⁶*Ludwig Maximilians University, 80539 Munich*
- ⁴⁷*Luther College, Decorah, Iowa 52101*
- ⁴⁸*University of Maribor, 2000 Maribor*
- ⁴⁹*Max-Planck-Institut für Physik, 80805 München*
- ⁵⁰*School of Physics, University of Melbourne, Victoria 3010*
- ⁵¹*University of Mississippi, University, Mississippi 38677*
- ⁵²*University of Miyazaki, Miyazaki 889-2192*
- ⁵³*Moscow Physical Engineering Institute, Moscow 115409*
- ⁵⁴*Moscow Institute of Physics and Technology, Moscow Region 141700*
- ⁵⁵*Graduate School of Science, Nagoya University, Nagoya 464-8602*
- ⁵⁶*Kobayashi-Maskawa Institute, Nagoya University, Nagoya 464-8602*
- ⁵⁷*Università di Napoli Federico II, 80055 Napoli*
- ⁵⁸*Nara Women's University, Nara 630-8506*
- ⁵⁹*National Central University, Chung-li 32054*
- ⁶⁰*National United University, Miao Li 36003*
- ⁶¹*Department of Physics, National Taiwan University, Taipei 10617*
- ⁶²*H. Niewodniczanski Institute of Nuclear Physics, Krakow 31-342*
- ⁶³*Nippon Dental University, Niigata 951-8580*
- ⁶⁴*Niigata University, Niigata 950-2181*
- ⁶⁵*Novosibirsk State University, Novosibirsk 630090*
- ⁶⁶*Osaka City University, Osaka 558-8585*
- ⁶⁷*Pacific Northwest National Laboratory, Richland, Washington 99352*
- ⁶⁸*Panjab University, Chandigarh 160014*
- ⁶⁹*Peking University, Beijing 100871*
- ⁷⁰*University of Pittsburgh, Pittsburgh, Pennsylvania 15260*
- ⁷¹*Punjab Agricultural University, Ludhiana 141004*
- ⁷²*Research Center for Nuclear Physics, Osaka University, Osaka 567-0047*
- ⁷³*Theoretical Research Division, Nishina Center, RIKEN, Saitama 351-0198*
- ⁷⁴*University of Science and Technology of China, Hefei 230026*
- ⁷⁵*Showa Pharmaceutical University, Tokyo 194-8543*
- ⁷⁶*Soongsil University, Seoul 156-743*
- ⁷⁷*University of South Carolina, Columbia, South Carolina 29208*
- ⁷⁸*Stefan Meyer Institute for Subatomic Physics, Vienna 1090*
- ⁷⁹*Sungkyunkwan University, Suwon 440-746*
- ⁸⁰*School of Physics, University of Sydney, Sydney, New South Wales 2006*
- ⁸¹*Department of Physics, Faculty of Science, University of Tabuk, Tabuk 71451*
- ⁸²*Tata Institute of Fundamental Research, Mumbai 400005*
- ⁸³*Excellence Cluster Universe, Technische Universität München, 85748 Garching*
- ⁸⁴*Department of Physics, Technische Universität München, 85748 Garching*
- ⁸⁵*Department of Physics, Tohoku University, Sendai 980-8578*
- ⁸⁶*Earthquake Research Institute, University of Tokyo, Tokyo 113-0032*

⁸⁷Department of Physics, University of Tokyo, Tokyo 113-0033

⁸⁸Tokyo Institute of Technology, Tokyo 152-8550


⁸⁹Tokyo Metropolitan University, Tokyo 192-0397

⁹⁰Virginia Polytechnic Institute and State University, Blacksburg, Virginia 24061

⁹¹Wayne State University, Detroit, Michigan 48202

⁹²Yamagata University, Yamagata 990-8560

⁹³Yonsei University, Seoul 120-749

 (Received 15 October 2018; revised manuscript received 8 January 2019; published 21 February 2019)

We report the first observation of the double strange baryon $\Xi(1620)^0$ in its decay to $\Xi^-\pi^+$ via $\Xi_c^+ \rightarrow \Xi^-\pi^+\pi^+$ decays based on a 980 fb^{-1} data sample collected with the Belle detector at the KEKB asymmetric-energy e^+e^- collider. The mass and width are measured to be $1610.4 \pm 6.0(\text{stat})_{-4.2}^{+6.1}(\text{syst}) \text{ MeV}/c^2$ and $59.9 \pm 4.8(\text{stat})_{-7.1}^{+2.8}(\text{syst}) \text{ MeV}$, respectively. We obtain 4.0σ evidence of the $\Xi(1690)^0$ with the same data sample. These results shed light on the structure of hyperon resonances with strangeness $S = -2$.

DOI: [10.1103/PhysRevLett.122.072501](https://doi.org/10.1103/PhysRevLett.122.072501)

The constituent quark model has been very successful in describing the ground states of the flavor SU(3) octet and decuplet baryons [1–3]. However, some of the observed excited states do not agree well with the theoretical prediction. It is thus important to study such unusual states, both to probe the limitation of the quark models and to spot unrevealed aspects of the quantum-chromodynamics (QCD) description of the structure of hadron resonances. Intriguingly, the Ξ resonances with strangeness $S = -2$ may provide important information on the latter aspect.

The quantum numbers of several nucleons and $S = -1$ hyperon resonances have been measured. Recently, there has been significant progress in the experimental study of charmed baryons by the Belle, BABAR, and LHCb Collaborations. In contrast, only a small number of Ξ states have been measured [1]. Neither the first radial excitation with the spin parity of $J^P = \frac{1}{2}^+$ nor a first orbital excitation with $J^P = \frac{1}{2}^-$ has been identified. Determination of the mass of the first excited state provides a vital test of our understanding of the structure of Ξ resonances. One candidate for the first excited state is the $\Xi(1690)$, which has a three-star rating on a four-star scale [1]. Another candidate is the $\Xi(1620)$, with a one-star rating [1]. If the $\frac{1}{2}^-$ state is found, it will be the doubly strange analogue to the $\Lambda(1405)$ state, which has been postulated as a candidate meson-baryon molecular state or a pentaquark [4].

Experimental evidence for the $\Xi(1620) \rightarrow \Xi\pi$ decay was reported in K^-p interactions in the 1970s [5–7]. The mass and width measurements are consistent but have large statistical uncertainties. The most recent study, in 1981, has not found this resonance [8]. There is a lingering theoretical

controversy about the interpretation of the $\Xi(1620)$ and $\Xi(1690)$ states [9–16], extending from their assignment in the quark model to their existence. This would be addressed with new high-quality experimental results for the first excited state with $S = -2$. The hadronic decays of charmed baryons governed by the $c \rightarrow s$ quark transition are a good laboratory to probe these strange baryons.

In this Letter, we study the decay $\Xi_c^+ \rightarrow \Xi^{*0}\pi^+$, $\Xi^{*0} \rightarrow \Xi^-\pi^+$ based on a data sample collected with the Belle detector at the KEKB asymmetric-energy e^+e^- (3.5 on 8 GeV) collider [17]. The charge conjugate mode is included throughout this Letter. The sample corresponds to an integrated luminosity of 980 fb^{-1} . The major part of the data was taken at the $\Upsilon(4S)$ resonance; in addition, smaller integrated luminosity samples were collected off resonance and at the $\Upsilon(1S)$, $\Upsilon(2S)$, $\Upsilon(3S)$, and $\Upsilon(5S)$. We use a Monte Carlo (MC) simulation sample to characterize the mass resolution, detector acceptance, and invariant mass distribution in the available phase space. The MC samples are generated with EVTGEN [18], and the detector response is simulated with GEANT3 [19].

The Belle detector is a large-solid-angle magnetic spectrometer that consists of a silicon vertex detector (SVD), a 50-layer central drift chamber (CDC), an array of aerogel threshold Cherenkov counters (ACC), a barrel-like arrangement of time-of-flight scintillation counters (TOF), and an electromagnetic calorimeter comprised of CsI(Tl) crystals (ECL); all these components are located inside a superconducting solenoid coil that provides a 1.5 T magnetic field. The detector is described in detail elsewhere [20]. Two inner detector configurations were used. A 2.0 cm radius beam pipe and a 3-layer SVD was used for the first sample of 156 fb^{-1} , while a 1.5 cm radius beam pipe, a 4-layer SVD and a small-cell inner CDC were used to record the remaining 824 fb^{-1} [21].

We reconstruct the Ξ_c^+ via the $\Xi_c^+ \rightarrow \Xi^-\pi^+\pi^+$, $\Xi^- \rightarrow \Lambda\pi^-$, $\Lambda \rightarrow p\pi^-$ decay channel. Final-state charged

particles, p and π^\pm , are identified using the information from the tracking (SVD, CDC) and charged-hadron identification (CDC, ACC, TOF) systems combined into likelihood ratios $\mathcal{L}(i:j) = \mathcal{L}_i/(\mathcal{L}_i + \mathcal{L}_j)$, where $i, j \in \{p, K, \pi\}$. The π^\pm particles are selected by requiring $\mathcal{L}(\pi:K) > 0.6$; this has about 90% efficiency. The criteria $\mathcal{L}(p:\pi) > 0.6$ and $\mathcal{L}(p:K) > 0.6$ are required for proton candidates from the Λ . The Λ particles are reconstructed from $p\pi^-$ pairs with about 98% efficiency. The three-momentum of the Λ is combined with that of a π^- track to reconstruct the helix trajectory of the Ξ^- candidate; this helix is extrapolated back toward the interaction point. A vertex fit is applied to the $\Xi^- \rightarrow \Lambda\pi^-$ decay and the χ^2 is required to be less than 50. We retain Ξ^- candidates whose mass is within $\pm 3.0 \text{ MeV}/c^2 (\pm 3\sigma)$ of the nominal Ξ^- mass. Then, we combine the Ξ^- with two π^+ candidates, where the pion with the lower (higher) momentum is labeled π_L^+ (π_H^+). The closest distance between the π^+ track and the nominal e^+e^- interaction point must satisfy $|dz| < 1.3 \text{ cm}$ along the beam direction, and $|dr| < 0.16(0.13) \text{ cm}$ in the transverse plane for π_L^+ (π_H^+) for both π_L^+ and π_H^+ . A vertex fit is applied to the $\Xi_c^+ \rightarrow \Xi^- \pi^+ \pi^+$ decay. The χ^2 is required to be less than 50. To purify the Ξ_c^+ samples, the scaled momentum $x_p = p_{\text{c.m.}}/\sqrt{\frac{1}{4}s - m(\Xi_c^+)^2}$ is required to exceed 0.5, where $p_{\text{c.m.}}$ is the momentum of Ξ_c^+ in the e^+e^- center-of-mass system, s is the squared total center-of-mass energy, and $m(\Xi_c^+)$ is the Ξ_c^+ nominal mass. We retain Ξ_c^+ candidates that satisfy $|M(\Xi^- \pi^+ \pi^+) - m(\Xi_c^+)| < 12.7 \text{ MeV}/c^2$. The region $30.0 \text{ MeV}/c^2 < |M(\Xi^- \pi^+ \pi^+) - m(\Xi_c^+)| < 55.4 \text{ MeV}/c^2$ defines the sideband for estimation of the combinatorial background.

The $M(\Xi^- \pi_L^+)$ and $M(\Xi^- \pi_H^+)$ distributions of the final sample are shown in Fig. 1(a). Peaks corresponding to $\Xi(1530)^0$, $\Xi(1620)^0$, and $\Xi(1690)^0$ are observed in the $M(\Xi^- \pi_L^+)$ distribution. A reflection due to $\Xi(1530)^0$ decays is seen around $2.2 \text{ GeV}/c^2$ in $M(\Xi^- \pi_H^+)$. The hatched histograms are the distributions of the Ξ_c^+ sideband events, where only the $\Xi(1530)^0$ is observed. The Dalitz plot of

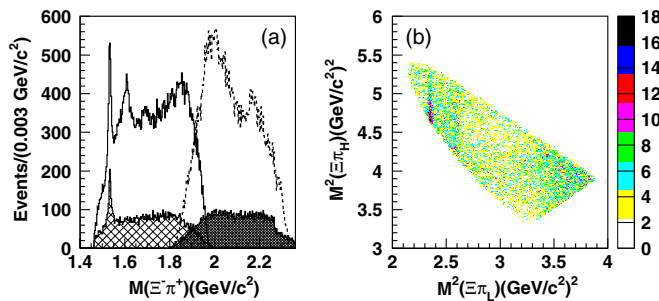


FIG. 1. (a) The $\Xi^- \pi_L^+$ (solid) and $\Xi^- \pi_H^+$ (dashed) invariant mass distributions in the Ξ_c^+ signal region, as well as the corresponding distributions (hatched) in the Ξ_c^+ sideband region. (b) The Dalitz distribution for $\Xi_c^+ \rightarrow \Xi^- \pi_L^+ \pi_H^+$.

$M^2(\Xi^- \pi_L^+)$ vs $M^2(\Xi^- \pi_H^+)$ is shown in Fig. 1(b). The cluster of events due to the $\Xi(1530)^0$ is seen. The region $4.3\text{--}5.3 (\text{GeV}/c^2)^2$ in $M^2(\Xi^- \pi_H^+)$ contains the $\Xi(1620)^0$ and $\Xi(1690)^0$ signals. There are currently no known particles with a mass in the range of $2.1\text{--}2.3 \text{ GeV}/c^2$ that would decay into $\Xi\pi$. Such massive particles would decay predominantly into a three-particle final state such as $\Xi\pi\pi$. The peaks around 1.60 and $1.69 \text{ GeV}/c^2$ in $M(\Xi^- \pi_L^+)$ are interpreted as the $\Xi(1620)^0$ and $\Xi(1690)^0$ resonances. We see an unknown structure in the range $1.8\text{--}2.1 \text{ GeV}/c^2$ in $M(\Xi^- \pi^+)$. These events are expected to be due to resonances such as $\Xi(1820)^0$, $\Xi(1950)^0$, and $\Xi(2030)^0$.

The correction of the event-reconstruction efficiency is applied to the mass spectrum. To calculate this efficiency, we generate MC events for the nonresonant three-body decay $\Xi_c^+ \rightarrow \Xi^- \pi^+ \pi^+$ with a uniform distribution in phase space. The efficiency is the number of events surviving the selections divided by the total number of generated events, and is measured as a function of $M(\Xi^- \pi_L^+)$; the resulting efficiency is from 0.082 to 0.097 and shows a nearly flat distribution in $M(\Xi^- \pi_L^+)$. The mass distribution is divided by this efficiency and is normalized by the total number of events.

We perform a binned maximum-likelihood fit to the efficiency-corrected $M(\Xi^- \pi_L^+)$ distribution. The fit is applied for the data samples in the signal region and the sideband region simultaneously. The fitting range is restricted to $(1.46, 1.76) \text{ GeV}/c^2$ to avoid inclusion of the unknown structure between 1.8 and $2.1 \text{ GeV}/c^2$. The fitting function for the mass spectrum in the signal region includes resonances due to the $\Xi(1530)^0$, $\Xi(1620)^0$, and $\Xi(1690)^0$, a nonresonant contribution, and the combinatorial background. The fitting function for the mass spectrum in the sideband region includes the $\Xi(1530)^0$ signal and the combinatorial background. The shape of the fitting function for the combinatorial backgrounds is common for the mass spectra in the signal region and the sideband region, and is made by a function with a threshold: $u^a \exp(ub) + cu$, where $u = 1 - [(2 - M)/(2 - d)]^2$ and $M = M(\Xi^- \pi_L^+)$; a , b , c , and d are free parameters. We assume an S -wave nonresonant contribution, and generate the distribution from the MC simulation of $\Xi_c^+ \rightarrow \Xi^- \pi^+ \pi^+$ decays with a uniform distribution in phase space. The $\Xi(1620)^0$ signal is modeled with the S -wave relativistic Breit-Wigner function. The $\Xi(1530)^0$ and $\Xi(1690)^0$ signals are modeled with P - and S -wave relativistic Breit-Wigner functions convolved with a fixed Gaussian resolution function of width 1.38 and $2.04 \text{ MeV}/c^2$, respectively, as determined from the MC simulation. The width and mass of $\Xi(1530)^0$ and $\Xi(1620)^0$ particles are floated in the fit. The mass and width of the $\Xi(1690)^0$ are fixed in the fit to the values $(1686 \text{ MeV}/c^2$ and 10 MeV , respectively) measured by the WA89 Collaboration [22]. The interference between the $\Xi(1620)^0$ and the S -wave nonresonant

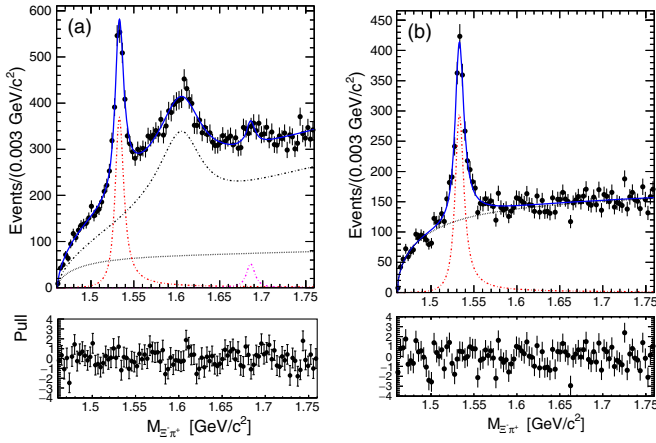


FIG. 2. (a) The $\Xi^- \pi_L^+$ invariant mass spectrum in the signal region (points with error bars), together with the fit result (solid blue curve) including the following components: $\Xi(1530)^0$ signal (dashed red curve), $\Xi(1690)^0$ signal (dot-dashed pink curve), $\Xi(1620)^0$ signal and nonresonant contribution (dot-dashed black curve), the combinatorial backgrounds (dotted black curve). The bottom plots show the normalized residuals (pulls) of the fits. (b) The $\Xi^- \pi_L^+$ invariant mass spectrum in the sideband region (points with error bars), together with the fit result (solid blue curve) including the following components: $\Xi(1530)^0$ signal (dashed red curve), and the combinatorial backgrounds (dotted black curve).

process is taken into account, and these are coherently added. We check the interference of the $\Xi(1690)^0$ to the S -wave nonresonant process and the $\Xi(1620)^0$ by applying the fit with the interference term, and it is negligible. Figure 2(a) and 2(b) show the $\Xi^- \pi_L^+$ mass spectrum in the signal region and the sideband region with the fitting result, respectively. The χ^2/ndf (where ndf is the number of degrees of freedom) is 66/86. For the $\Xi(1620)^0$ and the $\Xi(1690)^0$ resonance, fits are repeated by fixing each yield to zero; the resulting difference in log-likelihood with respect to the nominal fit and the change of the number of degrees of freedom are used to obtain the statistical significance. Taking the systematic uncertainties mentioned later into account, the signal significance of the $\Xi(1620)^0$ is obtained to be 25σ . The statistical significance of the $\Xi(1690)^0$ is 4.5σ . When the P -wave-only relativistic Breit-Wigner function with fixed mass and width is used as the fitting function, the significance is 4.0σ . When the S -wave-only relativistic Breit-Wigner function with the floated mass and width is used, the significance is 4.6σ . We take the minimum value of 4.0σ as the significance including the systematic uncertainty. The measured mass and width of $\Xi(1530)^0$ are $1533.4 \pm 0.4 \text{ MeV}/c^2$ and $11.2 \pm 1.5 \text{ MeV}$, respectively. The measured mass and width of $\Xi(1620)^0$ are $1610.4 \pm 6.0 \text{ MeV}/c^2$ and $60.0 \pm 4.8 \text{ MeV}$, respectively. The mass resolution (σ) at $1600 \text{ MeV}/c^2$ is $1.6 \text{ MeV}/c^2$ as determined from the

TABLE I. Systematic uncertainties for the mass and the width of $\Xi(1620)^0$.

Source	Mass (MeV/c^2)	Width (MeV)
Mass scale	-1.5	-2.7
Mass shape of $\Xi(1620)$	+4.5	+1.8
Mass shape of $\Xi(1690)$	+2.3	+1.7
Nonresonant contribution	-2.3	+0.3/ - 3.8
Interference with $\Xi(1690)$	+1.3	-5.2
Bin size	± 3.1	± 1.3
Total	+6.1 -4.2	+2.8 -7.1

MC simulation. The width of the $\Xi(1620)^0$ is 59.9 MeV after incorporating this mass resolution.

We itemize the systematic uncertainties on the mass and width of the $\Xi(1620)^0$ resonance in Table I. The mass scale and width is checked by comparing the reconstructed mass of the $\Xi(1530)^0$ in the $\Xi^- \pi^+$ channel with the nominal mass. The differences of the mass and width are $-1.5 \text{ MeV}/c^2$ and -2.7 MeV , respectively. We then generate and simulate $\Xi_c^+ \rightarrow \Xi^* \pi^+$, $\Xi^* \rightarrow \Xi^- \pi^+$ events and analyze them by the same program as for the real data; the mass scale is checked by comparing the reconstructed mass of Ξ^* with the generated mass. Here, the difference of the mass is $-0.2 \text{ MeV}/c^2$ and the difference of the width is less than the statistical error. The systematic uncertainties due to the mass shapes of the $\Xi(1620)^0$ and $\Xi(1690)^0$ are obtained by the fitting their masses and widths after switching each to the P -wave relativistic Breit-Wigner function instead of the nominally used S -wave form. Deviation from pure phase space for the nonresonant contribution is possible, and we estimate this systematic uncertainty by multiplying the nominal phase-space distribution with a third-order polynomial passing the kinematical lower bound of $M(\Xi^- \pi^+)$ and refitting. The systematic uncertainty from possible interference between the $\Xi(1690)^0$ and the nonresonant component is estimated by comparing the fit results with and without interference applied. The nominal bin width of the mass spectrum is $3.0 \text{ MeV}/c^2$. We determine its systematic uncertainty by changing the bin size from 2.5 to $3.5 \text{ MeV}/c^2$ and refitting.

All of the above sources are uncorrelated, so the total systematic uncertainties are calculated by summing them in quadrature.

We refit the data using a function that excludes the interference between $\Xi(1620)^0$ and the S -wave nonresonant process. The χ^2/ndf is 80/87, which is worse than the nominal fit result (66/86). The refitted mass and width of the $\Xi(1620)^0$ are $1601.2 \pm 1.5 \text{ MeV}/c^2$ and $63.6 \pm 8.7 \text{ MeV}$, respectively.

For the first time, the $\Xi(1620)^0$ particle is observed in its decay to $\Xi^- \pi^+$ via $\Xi_c^+ \rightarrow \Xi^- \pi^+ \pi^+$ decays. The number of $\Xi(1620)^0$ events is 2 orders of magnitude larger than that in

previous experiments. The measured mass and width of the $\Xi(1620)^0$ are consistent with the results of previous measurements within the large uncertainties of the latter and are much more precise. The width of the $\Xi(1620)^0$ is somewhat larger than that of the other Ξ^* particles [1].

The constituent quark models have predicted the first excited states of Ξ around 1800 MeV/ c^2 [3]; therefore, it is difficult to explain the structure of the $\Xi(1620)^0$ and $\Xi(1690)^0$ in this context. Instead, it implies that these states are candidates of a new class of exotic hadrons. We observe in the low-mass region two states with a mass difference of about 80 MeV/ c^2 : the $\Xi(1620)^0$ is strongly coupled to $\Xi\pi$ and the $\Xi(1690)^0$ to ΣK . The situation is similar to the two poles of the $\Lambda(1405)$ [4] and suggests the possibility of two poles in the $S = -2$ sector. Studying these states may explain the riddle about the $\Lambda(1405)$; consequently, the interplay between the $S = -1$ and $S = -2$ states can help resolve this longstanding problem of hadron physics.

The $\Xi(1620)^0$ and $\Xi(1690)^0$ particles are found in the decay of Ξ_c^+ while their signals are not seen in the sideband events of Fig. 1(a). These results offer a clue for understanding the quark structure of these exotic states. The result indicates that the hadronic decays of charmed baryons via charm-to-strange quark transitions are potentially a promising system for further studies of strange baryons [16].

We thank the KEKB group for the excellent operation of the accelerator; the KEK cryogenics group for the efficient operation of the solenoid; and the KEK computer group, and the Pacific Northwest National Laboratory (PNNL) Environmental Molecular Sciences Laboratory (EMSL) computing group for strong computing support; and the National Institute of Informatics, and Science Information NETwork 5 (SINET5) for valuable network support. We acknowledge support from the Ministry of Education, Culture, Sports, Science, and Technology (MEXT) of Japan, the Japan Society for the Promotion of Science (JSPS), and the Tau-Lepton Physics Research Center of Nagoya University; the Australian Research Council including Grants No. DP180102629, No. DP170102389, No. DP170102204, No. DP150103061, and No. FT130100303; Austrian Science Fund under Grant No. P 26794-N20; the National Natural Science Foundation of China under Contracts No. 11435013, No. 11475187, No. 11521505, No. 11575017, No. 11675166, No. 11705209; Key Research Program of Frontier Sciences, Chinese Academy of Sciences (CAS), Grant No. QYZDJ-SSW-SLH011; the CAS Center for Excellence in Particle Physics (CCEPP); the Shanghai Pujiang Program under Grant No. 18PJ1401000; the Ministry of Education, Youth and Sports of the Czech Republic under Contract No. LTT17020; the Carl Zeiss Foundation, the Deutsche

Forschungsgemeinschaft, the Excellence Cluster Universe, and the VolkswagenStiftung; the Department of Science and Technology of India; the Istituto Nazionale di Fisica Nucleare of Italy; National Research Foundation (NRF) of Korea Grants No. 2015H1A2A1033649, No. 2016R1D1A1B01010135, No. 2016K1A3A7A09005 603, No. 2016R1D1A1B02012900, No. 2018R1A2B3003 643, No. 2018R1A6A1A06024970, and No. 2018R1D1A1B07047294; Radiation Science Research Institute, Foreign Large-size Research Facility Application Supporting project, the Global Science Experimental Data Hub Center of the Korea Institute of Science and Technology Information and KREONET/GLORIAD; the Polish Ministry of Science and Higher Education and the National Science Center; the Grant of the Russian Federation Government, Agreement No. 14.W03.31.0026; the Slovenian Research Agency; Ikerbasque, Basque Foundation for Science, Basque Government (No. IT956-16) and Ministry of Economy and Competitiveness (MINECO) (Juan de la Cierva), Spain; the Swiss National Science Foundation; the Ministry of Education and the Ministry of Science and Technology of Taiwan; and the United States Department of Energy and the National Science Foundation.

-
- [1] M. Tanabashi *et al.* (Particle Data Group), *Phys. Rev. D* **98**, 030001 (2018).
 - [2] K. T. Chao, N. Isgur, and G. Karl, *Phys. Rev. D* **23**, 155 (1981).
 - [3] S. Capstick and N. Isgur, *Phys. Rev. D* **34**, 2809 (1986).
 - [4] T. Hyodo and D. Jido, *Prog. Part. Nucl. Phys.* **67**, 55 (2012).
 - [5] E. Briefel *et al.*, *Phys. Rev. D* **16**, 2706 (1977).
 - [6] A. de Bellefon, A. Berthon, P. Billoir, J. M. Brunet, G. Tristram, J. Vrana, B. Baccari, G. Poulard, D. Revel, and B. Tallini, *Nuovo Cimento* **28**, 289 (1975).
 - [7] R. T. Ross, T. Buran, J. L. Lloyd, J. H. Mulvey, and D. Radojicic, *Phys. Lett.* **38B**, 177 (1972).
 - [8] J. K. Hassall, R. E. Ansorge, J. R. Carter, W. W. Neale, J. G. Rushbrooke, D. R. Ward, B. Y. Oh, M. Pratap, G. A. Smith, and J. Whitmore, *Nucl. Phys.* **B189**, 397 (1981).
 - [9] U. Loring, B. Ch. Metsch, and H. R. Petry, *Eur. Phys. J. A* **10**, 447 (2001).
 - [10] A. Ramos, E. Oset, and C. Bennhold, *Phys. Rev. Lett.* **89**, 252001 (2002).
 - [11] C. Garcia-Recio, M. F. M. Lutz, and J. Nieves, *Phys. Lett. B* **582**, 49 (2004).
 - [12] Y. Oh, *Phys. Rev. D* **75**, 074002 (2007).
 - [13] M. Pervin and W. Roberts, *Phys. Rev. C* **77**, 025202 (2008).
 - [14] L. Y. Xiao and X. H. Zhong, *Phys. Rev. D* **87**, 094002 (2013).
 - [15] R. N. Faustov and V. O. Galkin, *Phys. Rev. D* **92**, 054005 (2015).
 - [16] K. Miyahara, T. Hyodo, M. Oka, J. Nieves, and E. Oset, *Phys. Rev. C* **95**, 035212 (2017).
 - [17] S. Kurokawa and E. Kikutani, *Nucl. Instrum. Methods Phys. Res., Sect. A* **499**, 1 (2003) and other papers included

- in this volume; T. Abe *et al.*, Prog. Theor. Exp. Phys. (**2013**) 03A001 and references therein.
- [18] D. J. Lange, Nucl. Instrum. Methods Phys. Res., Sect. A **462**, 152 (2001).
 - [19] R. Brun *et al.*, Report No. CERN DD/EE/84-1 (1984).
 - [20] A. Abashian *et al.* (Belle Collaboration), Nucl. Instrum. Methods Phys. Res., Sect. A **479**, 117 (2002); also see detector section in J. Brodzicka *et al.*, Prog. Theor. Exp. Phys. (**2012**) 4D001.
 - [21] Z. Natkaniec *et al.* (Belle SVD2 Group), Nucl. Instrum. Methods Phys. Res., Sect. A **560**, 1 (2006).
 - [22] M. I. Adamovich *et al.* (WA89 Collaboration), Eur. Phys. J. C **5**, 621 (1998).